We are IntechOpen,
the world's leading publisher of
Open Access books
Built by scientists, for scientists

6,900
Open access books available

185,000
International authors and editors

200M
Downloads

154
Countries delivered to

Our authors are among the

TOP 1%
most cited scientists

12.2%
Contributors from top 500 universities

CLARIVATE ANALYTICS
BOOK CITATION INDEX
INDEXED

WEB OF SCIENCE™

Selection of our books indexed in the Book Citation Index
in Web of Science™ Core Collection (BKCI)

Interested in publishing with us?
Contact book.department@intechopen.com

1

Application of Geophysical Methods to Waste Disposal Studies

Cristina Pomposiello, Cristina Dapeña, Alicia Favetto and Pamela Boujon
Instituto de Geocronología y Geología Isotópica (INGEIS, CONICET-UBA)
Argentina

1. Introduction

Geophysical methods provide information on the distribution of certain physical parameters in the sub-surface, which can be linked to the direct observations. Thus it is called an indirect observation method and it does not provide a "photo" of the sub-surface but it suggests a model of the underground derived from interpreting the distribution of these physical parameters. Clay and granite, for example, have different densities, acoustic velocities, elastic parameters, electrical conductivities, magnetic susceptibilities, and dielectric constants. So, geophysical methods are designed to exploit some of the physical properties of a target feature that is in contrast with its host environment, e.g., the low density nature of a void is in contrast to the high density nature of surrounding bedrock, etc. Geophysics should never be a stand-alone tool, but complementary to direct observations, which provide geological/hydrogeological background information (such as some of those methods seen in Table 1).

There are two general types of geophysical methods: 1) active, which measure the sub-surface response to electromagnetic, electrical, and seismic energy generated by artificial sources; and 2) passive, which measure the earth's ambient magnetic, electrical, and gravitational fields. Geophysical instruments are designed to map spatial variations in the physical properties of the Earth. A gravimeter, for example, is designed to measure spatial variations in the strength of Earth's gravitational field.

Sanitary landfill is the most common way to eliminate solid urban wastes. They have a heterogeneous structure due to random origin of the disposed waste. Geophysical methods are particularly valuable because they are non-destructive and non-invasive. An important problem associated with this practice is leachate production and the related groundwater contamination. Leachate electrical conductivity is often much higher than that of natural groundwater and it is this large contrast that enables contamination plumes to be detected using geophysical methods.

Ground Penetrating Radar (GPR) and Electrical methods such as Electrical Tomography (ET) and Vertical Electrical Sounding (VES) have been found to be especially useful for these kinds of environmental studies, due to the conductive nature of most contaminants, and they can be important tools for the detection and mapping of landfills, trenches, buried wastes and drums, or other underground structures.

Geophysical Method	Measured Parameter	Physical Property	Physical Property Model	Applications
Electrical resistivity	Potential difference and induce current	Electrical resistivity	Electrical resistivity model	Determine depth and thickness of geological layers.
Induced polarization (IP)	Polarization voltages or frequency dependent ground resistance	Electrical capacity	Electrical capacity model	Determine electrical conductive targets such as clay content (or metallic)
Ground penetrating radar (GPR)	Travel times and amplitudes of EM waves.	Dielectric constant, magnetic permeability and electrical conductivity.	EM velocity model	Detect both metallic and non-metallic targets
Magnetics	Spatial variations in the strength of magnetic field of the Earth	Magnetic susceptibility and remanent magnetization	Model depicting spatial variations in the magnetic susceptibility of subsurface.	Map geological structures and detect buried drums, tanks, and other metal objects
Gravity	Spatial variations in the strength of gravitational field of the Earth	Bulk density	Model depicting spatial variations in the density of sub-surface	Determine any geologic structure involving mass variations.

Table 1. Geophysical methods employed for environmental investigations.

1.1 Sub-surface electrical resistivity

Several conduction mechanisms are possible in typical sub-surface material. They are: a) electronical conduction, b) semiconductors and c) ionic conduction in liquids.

a.   Electronic conduction occurs in pure metals. In this mechanism the charge carriers are electrons and their high mobility gives a very low resistivity (< 10^{-8} ohm-m).

b.   Semiconduction occurs in minerals such as sulphides and typically in igneous rocks. In this case the charge carries are electrons, ions or holes. Compared to metals, the mobility and number of charge carriers are lower and thus the resistivity higher (typically 10^{-3} to 10^{-5} ohm-m).

c.   Ionic conduction in liquids (or electrolytic conduction) occurs when current flows via the movement of ions in aqueous fluids or molten materials. The resistivity of rocks is greatly dependent on the degree of fracturing and the percentage of the fractures filled with fluids. Igneous and metamorphic rocks normally have higher resistivity values compared with sedimentary rocks (typically 1 to 100 ohm-m), which are usually more porous and have higher water content. The resistivity values are largely dependent on the porosity of the rocks and the salinity of the ground water.

Electrical resistivity distribution is useful for determining shallow and deep geological and hydrogeological conditions. Geoelectrical surveys are commonly used in hydrogeological, mining and geotechnical investigations. More recently, it has been used for environmental surveys (Loke, 1999). The resistivity data can be used to identify, delineate and map the sub-surface defining such things as electrical conductor contamination plumes, lithologic units with clay, the salt water/fresh water interface and the vadose zone.

The deposits in landfill sites have different origins, for example domestic and industrial wastes, soils and exhumed geological materials. They have a complex material composition; they are non-uniformly compacted and also have a non-uniform decomposition process, so their physical properties would present a wide range of variation. For example the electrical resistivity has values that range from 1.5 to 20 ohm-m in different landfills (Meju et al. 2000). Leachate is a liquid formed from decomposed waste and it can contain ground water and percolated rainwater. Inorganic pollutants increase liquid conductivity due the presence of dissolved salts. Consequently, the electrical resistivity of leachate is often very much lower than natural groundwater. For example, the fresh water has a resistivity around 200 ohm-m and the saline water has a resistivity of around 10 ohm-m. Other type of pollutants, such as organic compounds can reduce leachate conductivity.

1.2 Geoelectrical methods

The sub-surface resistivity distribution can be determined by making measurements on the ground surface. From these measurements, the true resistivity can be inferred. The ground resistivity is related to various geological parameters such as the mineral and fluid content, porosity and degree of water saturation in the rock.

The resistivity measurements are normally made using a man-made source of electrical current that is applied to the earth through grounded electrodes (C1 and C2 in Figure 1). The resulting potential field is measured along the ground using a second pair of electrodes (P1 and P2). The transmitting and receiving electrode pairs are referred to as dipoles. By varying the unit length of the dipoles as well as the distance between them, the horizontal and vertical distribution of electrical properties can be calculated. From the current (I) and voltage (V) values, the apparent resistivity (ρa) is calculated, $\rho a = k \, V \,/I$ where k is the geometrical factor which depends on the arrangement of the four electrodes.

The apparent resistivity is not the true resistivity of the surface, but this value equals that of the resistivity of homogeneous ground measured from the same electrode arrangement. From the apparent resistivity values it is possible obtain the true surface resistivity using an inversion method.

Fig. 1. A conventional four electrode array to measure the sub-surface resistivity.

1.2.1 1D Vertical Electrical Sounding (VES)

The vertical electrical sounding is performed changing the electrode spacing over a common centre point. The electrical current is applied to A and B electrodes and the potential V is measured between M and N electrodes. The VES array consists of a series of the electrode combinations AMNB with gradually increasing distances between the electrodes for subsequent combinations. The Schlumberger array is shown in Figure 2. The depth of sounding increases with the distance between A and B electrodes.

VES provides measurements of apparent resistivity obtaining a sounding curve (Figure 3a), by plotting resistivity ρa against the half distance between the current electrodes (AB/2) with k= π (AO² - MN²/4)/MN. It is interpreted quantitatively to derive thickness and resistivity of sub-surface layers using the appropriate software which determines a depth-layer model of resistivity (1-D-model). It provides the vertical resistivity variation under the centre point and it is applicable to horizontally layered homogenous ground (Figure 3b).

This method is a very important tool employed in the geophysical exploration of the shallow sub-surface. The normal depth range that is investigated is from a few centimetres to a few hundred meters. These techniques are thus particularly applicable in groundwater, and environment characterizations. The distinction between mainly clayey/silty layers (aquitards) and dominantly sandy/gravely beds (aquifers) are specially distinguishable to determine. Furthermore, it can be used to determine saltwater intrusion and contaminated plumes
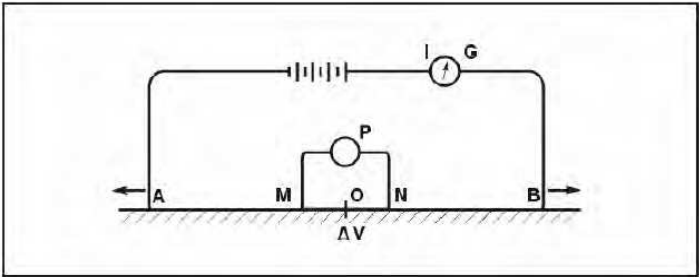

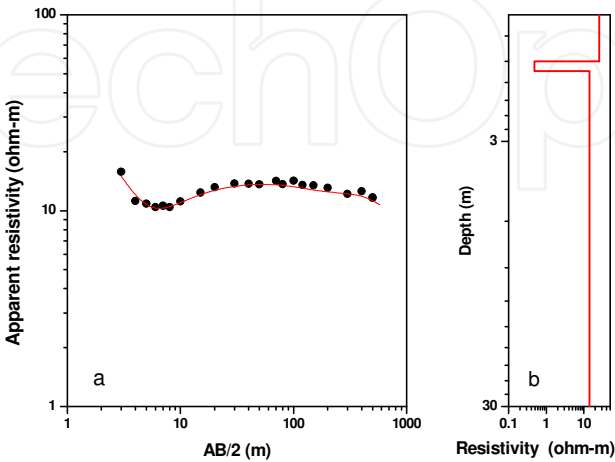Fig. 2. Schlumberger array, depth of sounding controlled by the distance between A and B.

Fig. 3. a) Sounding curve, apparent resistivity vs. the half distance between the current electrodes. b) 1D model, depth vs. resistivity (log-log, representation).

1.2.2 2D Electrical Tomography (ET)

2D imaging assumes low variation of the third dimension. 3D surveys involve large amount of measurements and more data processing.

In an electrical tomography an array of regularly – spaced electrodes is deployed. They are connected to a central control unit via multi-core cables. The common arrays used are dipole-dipole, Schumberger and Wenner, depending on application and the resolution desired (Loke, 1999). The advantages and disadvantages of these arrays will be used to choose the appropriate configuration in each case. The dipole-dipole array is present in Figure 4. In this case, the spacing between the current electrodes pair, AB is given as "a" which is the same as the distance between the potential electrodes pair MN. The same process is repeated for measurements with different spacing ("2**a**" to "na"). The apparent resistivity is calculated with k = π(n(n+1)(n+2)a, where n is the level. The median depth of investigation of this array also depends on the "**n**" factor, as well as the "**a**".
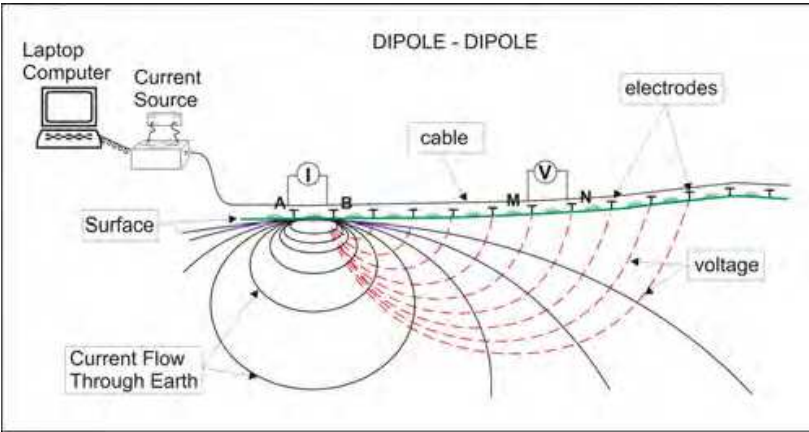

Fig. 4. Multi-channel dipole-dipole surveys.

Resistivity data are then recorded via complex combinations of current and potential electrode pairs to build up a pseudo cross-section of apparent resistivity beneath the survey profile (Figure 5).
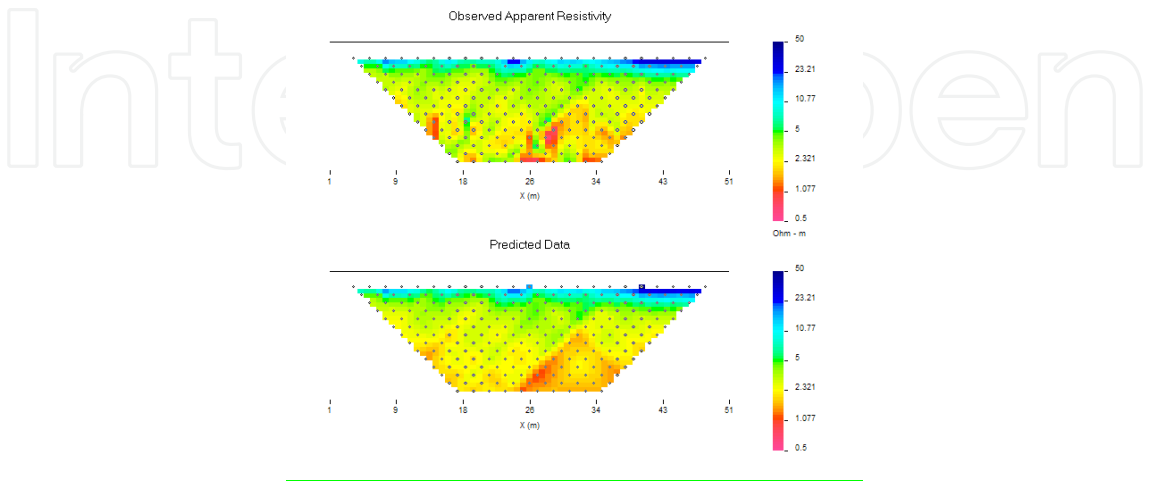

Fig. 5. An example of observed apparent resistivity (a = 2 m and 231 data) and predicted data by an inversion method.

Electrical tomography has many applications in geology, hydrogeology and environmental studies, for example:

a.   Determination of the depth and thickness of geological strata.
b.   Detection of lateral changes and locating anomalous geological conditions
c.   Locating buried wastes (e.g., locate landfill)
d.   Mapping saltwater intrusion and contaminated plumes.

This electrical resistivity imaging survey is widely used to control the depth extent and geometry of the landfill. Frequent monitoring landfill leachate with this technique could allow early leak detection.

1.2.3 GPR

Ground penetrating radar (GPR) uses pulsed high frequency radio waves (10 to 2000 MHz) to probe the sub-surface without disturbing the ground. Energy is radiated down-ward into the ground from a transmitter and is reflected back to a receiving antenna (Figure 6). The reflected signals are recorded continuously as the GPR is pulled over the ground surface and provides a real-time cross section or image of the subsurface (Figure 7). GPR can be used in a great variety of materials such as rock, soil, ice, fresh water and road surfaces.
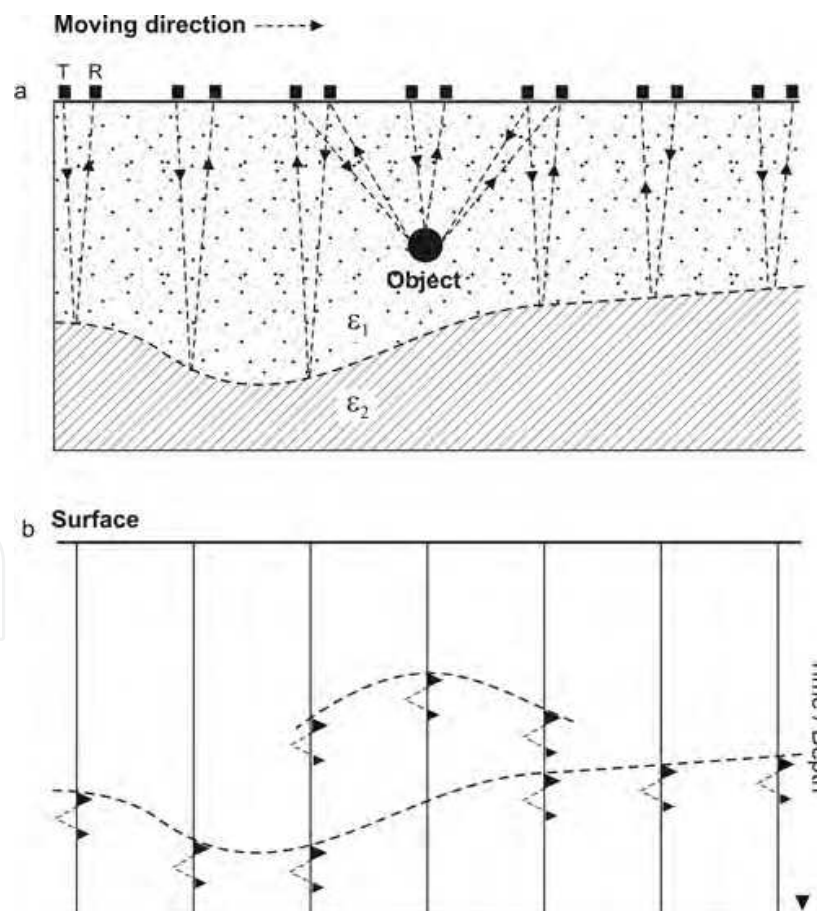

Fig. 6. a) Travel paths of the electromagnetic waves in a medium with two different dielectric proprieties and a buried object.   b) Travel times of the reflections. It is a function of the layer thickness and the velocities. The isolated body presents a hyperbola.

In this method the measured parameters are the travel time and amplitudes of reflected pulsed electromagnetic energy and they depend on physical properties such as the dielectric constant and the conductivity of the material. Essentially, a reflection occurs when there is a change in the dielectric constant of materials in the sub-surface (Table 2). The dielectric constant is defined as the capacity of a material to store a charge when an electric field is applied relative to the same capacity in vacuum, and can be computed as: $\varepsilon_r = (c/v)^2$, where: ε_r = the relative dielectric constant, **c** = the speed of light (30 cm/nanosecond), and **v** = the velocity of electromagnetic energy passing through the material.

The principles involved, in this method, are similar to reflection seismology except that electromagnetic energy is used instead of acoustic energy.
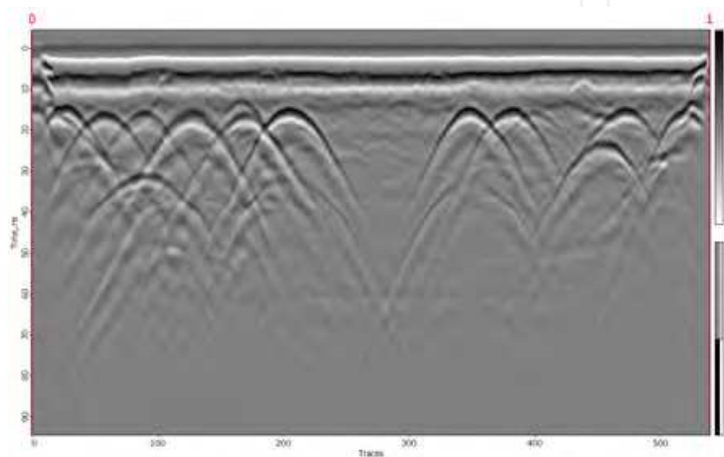

Fig. 7. Example of a GPR radargrama.

Material	Dielectric relative permittivity	Conductivity (mS/m)	Velocity (m/ns)	Attenuation (dB/m)
Air	1	0	0.3	0
Distillate water	80	0.001	0.033	0.002
Fresh water	80	0.5	0.033	0.1
Sea water	80	3000	0.01	1000
Dry sand	3-5	0.01	0.15	0.01
Wet sand	20-30	0.1-1	0.06	0.03-0.3
Limestone	4-8	0.5-2	0.12	0.4-1
Shale	5-15	1-100	0.09	1-100
Silt	5-30	1-100	0.07	1-100
Clay	5-40	2-1000	0.06	1-300
Granite	4-6	0.01-1	0.13	0.01-1
Ice	3-4	0.01	0.16	0.01

Table 2. Relative dielectric permittivity (relative dielectric constant), conductivity, velocity and attenuation for different media.

The penetration depth of GPR is determined by the antenna frequency and the electrical conductivity of the sub-surface materials being profiled (Daniels, 2004) and the choice of working frequency is dependent on the depth of penetration. As conductivity increases, the

penetration depth also decreases. This is because the electromagnetic energy is more quickly converted into heat, causing a loss in signal strength at depth. Soils having high electrical conductivity rapidly attenuate radar energy, restrict penetration depths, and severely limit the effectiveness of GPR. The electrical conductivity of soils increases with increasing water, clay and soluble salt contents. Optimal depth penetration is achieved in ice where the depth of penetration can achieve several hundred metres. Good penetration is also achieved in dry sandy soils or massive dry materials such as granite, limestone, and concrete where the depth of penetration could be up to 15 metres.

The GPR has many applications in environmental studies, principally the characterization of abandoned landfills: thickness of the deposit, location of metal and non-metal objects (barrels, voids, etc.), soil profiles, groundwater level and contaminant plume.

The GPR has several advantages, for example: a) measurements are relatively easy to make, b) the lateral and vertical resolution is very high and c) the antenna may be pulled by hand or vehicle.

Due to the complexity of the fill materials of the landfill, GPR signals in landfills are very complex and difficult for interpretation, Also the principal limitation is the presence of clay-rich soil or saline groundwater which can reduce the exploration depth due to the attenuation the radar signal. However, GPR can be used as a secondary tool for some localized interested area where the GPR survey might be able to provide additional detailed information and it is easier to follow the contamination plume due to the attenuation the radar signal outside the landfill.

2. Case studies

This chapter presents the geophysical results of multidisciplinary projects at two urban solid wastes, one sites in the city of Gualeguaychú, Province of Entre Ríos (Pomposiello et al, 2009), and the other in the city of San Carlos de Bariloche, Province of Rio Negro (Pomposiello et al, 2008), Argentina. As part of an environmental project several tomographies using dipole-dipole electrode array, vertical sounding using Schlumberger electrode configurations and GPR profiles with 150 –500 MHz antennae were performed within and outside the landfills and they were interpreted using one-dimensional and bidimensional models. These studies such as electrical resistivity imaging and GPR techniques were used to locate and monitor leachate plumes in landfill sites.

2.1 Applied geophysical methods

2.1.1. Dipole-Dipole (DD)

Geoelectrical profiles were performed using the DD configuration with 21 electrodes (spaced a = 5 with n =1, ..., 18) to give a total profile length of 100 meters. The maximum depth to which the experimental data gives reliable information on the electrical resistivity of medium was estimated. The resistivity model was obtained from the data inversion using the DCINV2D algorithm of Oldemburg et al. (1993). We compared the results using half-space reference models of 0.001, 0.01 and 0.1 mS/m. The depth of investigation index (DOI) as defined by Oldenburg et al. (1994) was calculated using a reference model of 0.001 mS/m and a cut off = 0.5.

2.1.2 Vertical Electrical Sounding (VES)

For the evaluation of the electrical resistivity in the deeper layers **VES** were made using Schlumberger configuration with opening distance (AB) between 6 m and 1000 m, which allows a model to be found focused on the measuring point and a penetration of 200 m and 300 meters. Models were obtained using the inversion software IPIWIN (Bobachev et al., 2000).

2.1.3 Ground Penetrating Radar (GPR)

The GPR allowed the observation of the shallowest levels (less than 10 m) and to distinguish the boundary between the deposits of waste and the area which is in contact with leachate. The GPR profiles were performed with 500 MHz antennas (screened) and 150 MHz (air). The commercial program Prism version 2.01 by Radar System, Inc (http://www.radsys.lv, 2004) was used.

2.2 Relationship between electrical conductivity and hydrochemistry parameters

Chemical analyses of contaminated groundwater by leachate in different geographical regions demonstrated that groundwater electrical conductivity has a strong lineal correlation with total dissolved solids (TDS) and chloride content (Cl-) (Meju 2000 & his references)

The leachate composition varies with the age of the landfill, and as a result recent solid wastes have higher contents of organic acids, ammonium and total dissolved salts (TDS), accordingly their concentrations decrease when biodegradation begins. As a consequence, it is possible to estimate the age of the landfill using these measurements (Farquhar, 1989; Meju, 2000).

In addition, Meju (2000) indicates that measuring the electrical conductivity of the saturate substrate (σ_b) makes possible to predict the values of TDS applying the following equations:

$$\log \sigma_b = -0{,}3215 + 0{,}7093 * \log TDS \qquad (1)$$

$$\log \sigma_b = -0{,}333 + 0{,}6453 * \log TDS \qquad (2)$$

where: σ_b is expressed in mS/m and TDS in mg/L. Equations (1) and (2) determine the minimum and maximum values respectively

From TDS values it is possible to predict the water electrical conductivity (σ_w) and the chloride content using the following equations

$$\log TDS = 0{,}8 + 1{,}015 * \log \sigma_w \qquad (3)$$

$$\log Cl^- = -0{,}256 + 1{,}2 * \log \sigma_w \qquad (4)$$

where: σ_w is expressed in mS/m and the last parameters in mg/L.

These relationships were calculated in a sanitary landfill in Durban, South Africa (Bell & Jermy, 1995). Data from others landfills in Australia (Buselli et al., 1990) and Canada (Birks & Eyles, 1997) also show a similar lineal tendency to the Durban values.

The water content (W) can be calculated applying equation (1) and considering the stratum free of clay. (Yaramanci, 1994):

$$\sigma_b = \sigma_w * W^m \tag{5}$$

where: W is the water content in percentage of volume (vol %) and m is the cementation factor, which value is between 1,6 y 1,9.

Equation (2) was established for relatively homogeneous materials and it can be non valid for environments with solid wastes and significant quantities of conductors, metals and clay.

As a result, the age of landfills can be determined considering the relations and the changes in the concentration of chemical parameters of lixiviates such as Cl-, TDS, pH, between others (Farquhar, 1989; Meju, 2000).

2.3 Gualeguaychú landfill

2.3.1 Background

The study area corresponds to the actual municipal sanitary landfill of the city of Gualeguaychú in the Southern Entre Ríos Province, Argentina (Figure 8). The landfill is near the south border of the city. This city has a population of 80000, and it has numerous commercial, industrial and agricultural activities. The landfill operations were suspended eleven years ago and no environmental studies were performed to evaluate its actual state and outline the contamination zone. Currently, the operation of the waste deposit has been resumed by the Municipal Urban Hygiene Enterprise, which solicited an evaluation of the actual state of the old sanitary landfill.
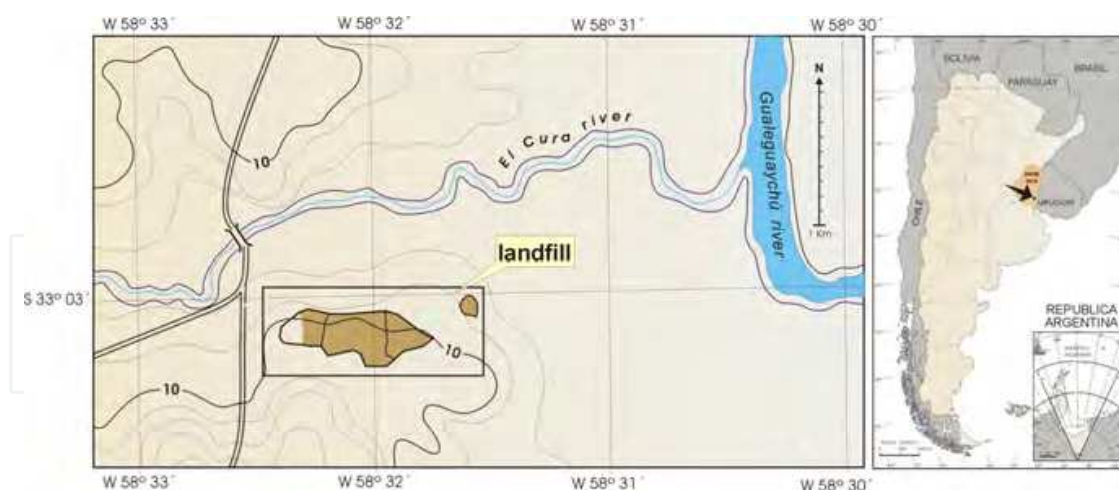

Fig. 8. Location of the Gualeguaychú landfill relevant to the Entre Rios province, Argentina.

At present, in Gualeguaychú there are two landfills overfilled and closed with different ages. The oldest and biggest was closed in 1998 and the smallest was closed in 2003. In the case of the first one, there are no records of its construction and it has neither leachate collection system nor a collection system for gases, although it is observed that the residues have been deposited in parallel cells. Now, a third landfill is in operation. This work only presents the results obtained in the first landfill.

The site of the landfill was initially used as a place of extraction of materials (ex quarry Irazusta), allowing the troughs to be used for the storage of solid waste. In particular, this site was an open dump where solid wastes were deposited and then covered by the excavated material (Figure 9). This material belongs to the Punta Gorda Group with lithology consisting of silt and clay with calcareous concretions and calcareous hardpan layers that appear at different levels (locally known as "tosca") and in the lower section the presence of clay is richer than the upper one and it also has some gypsum flake crystals. Wastes were not recycled prior to deposition and arranged in parallel modules (cells) of about 0.8 -1 m wide. Prezzi et al. (2005) estimated that the cells reach a maximum depth around 2 to 3 meters.

Fig. 9. A photo of the landfill landscape.

These landfills are located below the contour level of 10 m and the regional slope is approximately N-NE, toward the El Cura stream and the Gualeguaychú River with a very low gradient (Figure 8). The El Cura stream is the natural collector of the regional surface flow and always carries water generating a strong environmental impact due to the discharges of untreated sewage effluents of the city.

The boundaries and surface of the waste are irregular, following the geometry that comes from the alignment of cells and providing a soft and notable undulation. At the northern edge a channel is formed between the landfill and the road, where water accumulates. This deposit is divided into three parts, and between the central and west sector there is a waste-free zone which functions like a permanent course of water (stream W, Figure 10). The eastern sector is separated from the central one by a big area free of waste which also functions as an intermittent course of water (stream E, Figure 10) Both streams have a N-S direction carrying plenty of water after large precipitations. They discharge in an undefined way at the northern edge on the other side of the road forming flooded areas (Figure 10). The depressions between cells act as water reservoirs after rains.
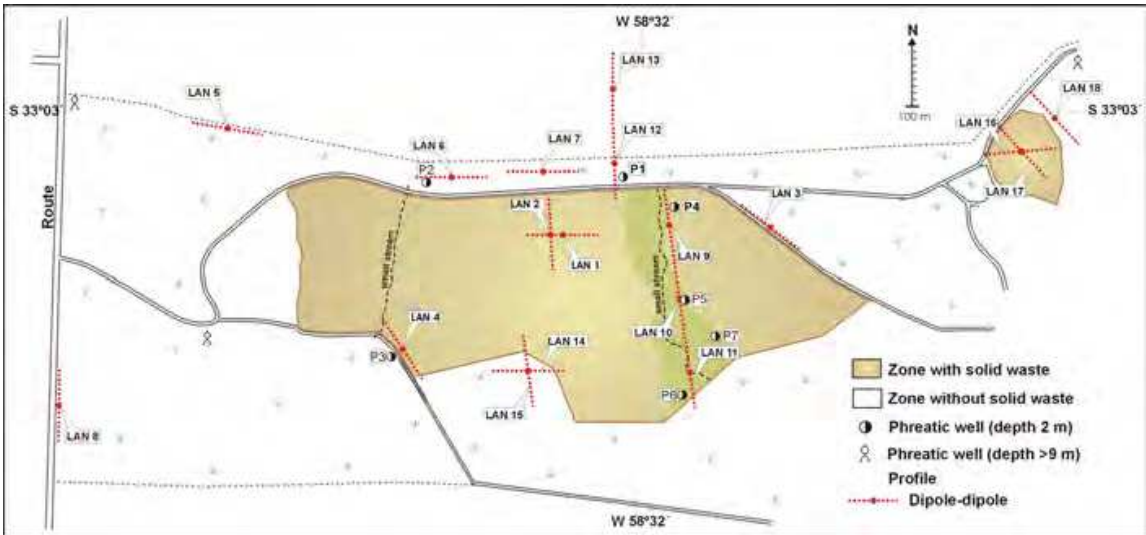
Fig. 10. A schematic map showing locations of dipole-dipole profiles (Lan) and phreatimeters (P).

2.3.2 Geological and hydrogeological setting

This region forms part of the Chaco-Paranense plain (Russo et al., 1979). The most important outcropping formations are described following Iriondo (1980) and Fili (2001) in Table 3.

AGE	UNIT	LITOLOGHY	THICKNESS (m)	HYDROGEOLOGIC BEHAVIOUR
Holocene	La Picada Formation	Silt and dark clay Fine quartzoses sandstones	1.5 to 3	Discontinuos unconfined aquifer, contains water table Poor water quality
Pleistocene	Punta Gorda Group	*Upper Section*: Brown Silt and clay with calcareous concretions and calcareous hardpan layers ("tosca") *Lower Section*: Clay with some gypsum crystals	20 to 40	Low productivity aquifer to aquitard Unconfined to semiconfined, contains water table Good to regular water quality
Upper Pliocene	Salto Chico Formation	Fine sandstones with silt and clay interlayers	60	Aquifer Excellent water quality

Table 3. Stratigraphic column.

2.3.3 Field work

Several geoelectrical studies, electrical tomography and vertical sounding using dipole-dipole and Schlumberger electrode configurations respectively and GPR profiles (antennas 150MHz -500MHz) were performed within and outside the landfill (Figure 9). Spatially coincident profiles for multi-electrode resistivity and GPR were carried out. A scheme of the

distribution of the profiles in the studied area is shown in Figure 9. The profiles Lan01, Lan02 and Lan04 are located inside the landfill area, Lan14 and Lan15 are partially located inside the landfill, Lan09, Lan10 and Lan11 are closed the stream E where there are no waste deposits, while the profiles Lan03, Lan05, Lan06, Lan07, Lan08, lan12 and Lan13 are outside the landfill and around the waste deposits (see Figure10).

During 2005, seven small wells (phreatimeters) were dug to 2.30 m below surface outside the landfill (Figure 10). They were cased with PVC tubes, capped at both extremes and had gravel filters at the bottom. These phreatimeters are used to control water level, chemical composition and isotope content. These wells are located, two in the south border, two in the north border and the others are between the central sector and east sector (Figure 10).

Phreatic levels respond faster to precipitation. The direction of the phreatic system flow is N-NE toward the El Cura stream and the Gualeguaychú River, both of effluent character. Temperature and electrical conductivity were periodically measured *in situ.*

2.3.4 Results

2D resistivity models corresponding to Lan01, Lan07 and Lan15 profiles were selected to discuss the most prominent results. These have been plotted between 0 and 20 m depth. It was considered that this depth is most appropriate to describe the surface geoelectrical characteristics and also to compare all the models to the same depth. Important conductivity anomalies have been detected below the waste disposal. The 2D model obtained within the landfill (Lan01, Lan02 and Lan04) shows a shallow layer with a thickness of 2 m to 3 m and a resistivity range from 100 to 1000 ohm-m, this layer represents the waste deposit (Figure 11). The second layer has a thickness of 4 m to 5 m and a low value of resistivity of 3 ohm-m to 6 ohm-m, which is attributed to the contaminated zone. The third layer has a thickness of more than 10 m and a resistivity of 15 ohm-meter. Below this depth is observed another conductive layer (5 ohm-m).
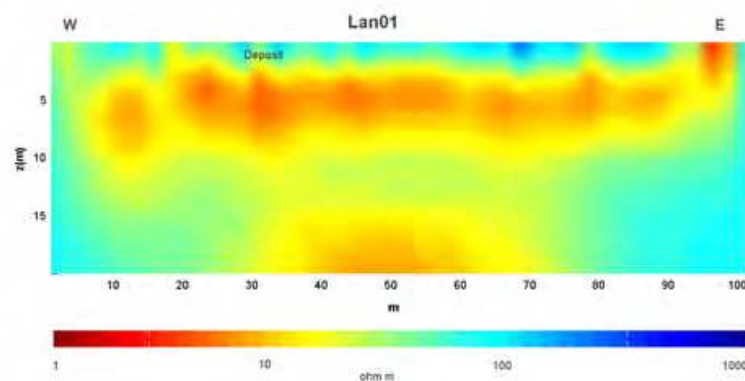

Fig. 11. 2D resistivity model up to 20 m deep obtained within the landfill (Lan01).

Several GPR profiles were performed inside and outside the landfill using a 150 MHz antenna and NS orientation covering approximately the entire length of the landfill and nearby outdoor areas.

The 2D electrical resistivity model and the GPR profile (150Mhz) of Lan02 are presented in Figures 12 and 13, and in this case the maximum depth of the electrical model was adapted

to the result of GPR. The reflectors are at the depths where the waste is observed in the electrical model and then the signal is attenuated significantly. A conductive body is observed in the same place where there is a shadow zone in the GPR profile. The high conductivity of materials is attributed to fluids rich in salts, which attenuate the radar waves, not allowing them to reach great depths.
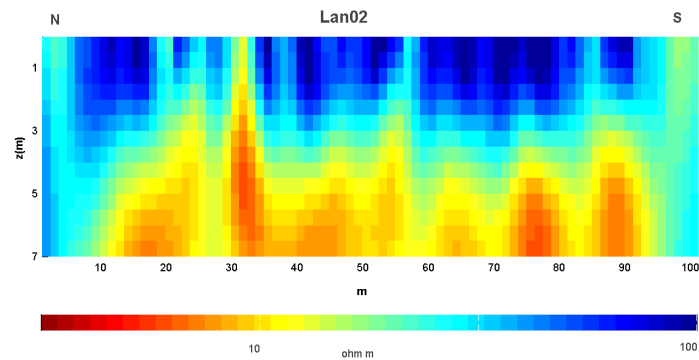
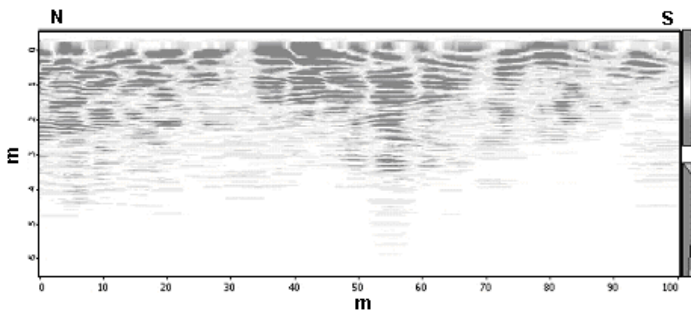

Fig. 12. 2D resistivity model up to 7m deep obtained within the landfill (Lan02).

Fig. 13. Radar image for the landfill up to 7m of depth (Lan 02).

The 2D models obtained to the north of the landfill and outside its boundaries (Lan05, Lan06 and Lan07) also show zones with low resistivity values in the first 5 meters. This resistivity anomaly can be explained as leachate and also by the presence of clay. The resistivity bodies found at a depth around 10 m have been interpreted as calcareous concretions and calcareous hardpan layers that appear at different levels in Punta Gorda sediments (locally known as "tosca") according to the geological description (Figure 14).
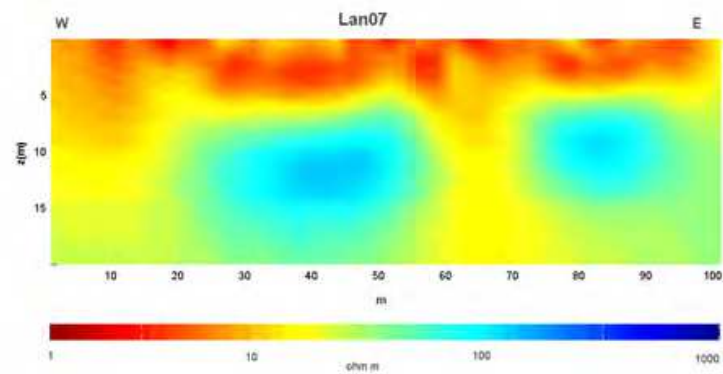

Fig. 14. 2D resistivity model up to 20 m deep obtained outside the landfill (Lan07).

Furthermore, the result corresponding to VES2 is presented in Figure 15. This sounding was performed close to Lan07 and shows similar results. It presents a conductive layer followed by another more resistive layer (15 ohm-m -25 ohm-m) extending up to near the 150 metres. The results are comparable because this model shows a first layer with a thickness of 2 m and resistivity of 4 ohm-m and a second layer with a thickness of 20 m and resistivity around 14 ohm-meters. Therefore, considering that the conductive layer is observed very superficially, the presence of leachate contamination is only restricted to the shallowest layer (<5 metres).
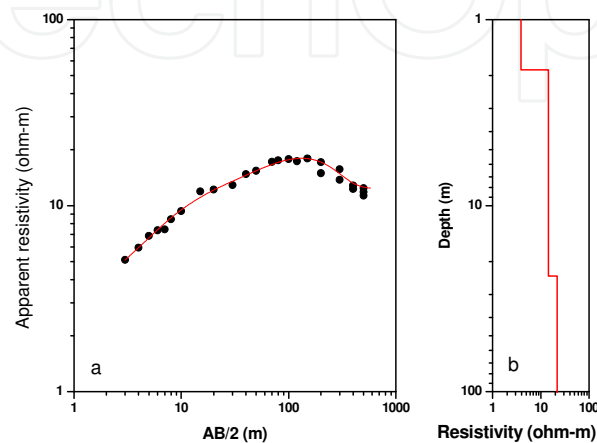
Fig. 15. a) Sounding curve, apparent resistivity vs. the half distance between the current electrodes. b) 1D model, depth vs. resistivity (log-log, representation).

Lan14 and Lan15 profiles are located in the southern part of the landfill. These profiles were made 30% over waste and the remaining 70% outside of the landfill. 2D electrical models show that in the surface and in the wastes the resistivity is high, about 250 ohm-m and a thickness around 3 meters. This result is consistent with Lan01, Lan02 and Lan04 models, which were discussed above showing that the resistivity is higher at the shallow depth where the wastes are deposited. Below them there is a conductive body with a resistive around 6 ohm-m which continues to the surface in the waste-free part. Where there is no waste the resistivity values varies between 3 ohm-m and 6 ohm-m with a thickness ranging from 2 m to 5 meters. Below this layer the resistivity ranges from 20 ohm-m to 40 ohm-meters (Figure 16).
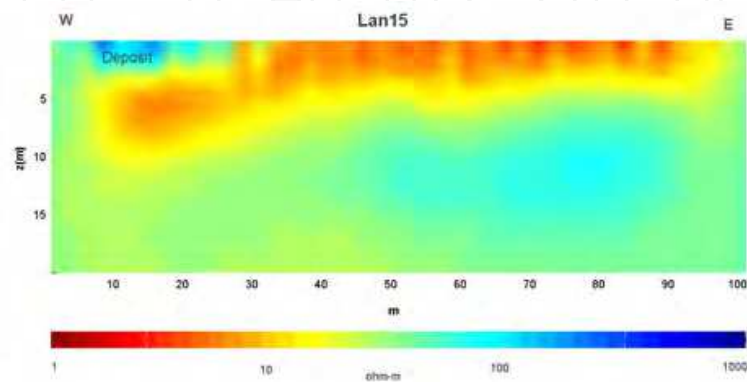

Fig. 16. 2D resistivity model up to 20 m deep obtained outside the landfill (Lan15).

2.3.4.1 Electrical conductivity of phreatic and surface water

The water electric conductivity measured in the phreatimeters installed near the border outside the landfill was related with the electric conductivity measured in the geoelectrical models obtained from tomography.

The electrical conductivity of phreatic, surface water and effluents were measured. Values measured in effluents and surface water bodies (accumulations between cells, small streams, temporary ponds, etc.) range between 170 μS/cm and 800 μS/cm and the measures in phreatimeters between 240 μS/cm and 8300 μS/cm. An increase is noticed from south to north and from SE to NW, in the direction of the regional flow. These values are strongly influenced by precipitations and a dilution is observed after each rain event (Dapeña, pers. Com.). In addition, effluents of the landfill show a fast response to the influence of precipitations.

2.3.4.2 Calculations of hydrochemical parameters

Table 4 shows the hydrochemical parameters calculated for the oldest landfill. The depth of the minimum resistivity was determined in the central part of the model (x=50m) of profiles Lan01, Lan02 and Lan04. In the case of Lan14 and Lan15 the analysis was only made in the section of the profile which contains solid wastes and the depth of the minimum resistivity was established.

The procedures illustrate by Meju (2000) were used for the calculations and the hydrochemical parameters are shown in Table 4.

The results show the values calculated using equation (2) are slightly more than double those calculated using equation (1).

Although the results presented in Table 4 are approximate, these values can be considered as maximum and minimum values of prediction in this study and are useful for evaluating the current environmental conditions. It must be taken into account that these results are an approximation and also that the parameters depend upon the leachate composition, infiltration, waste types and geological materials.

The age of this landfill was inferred using the minimum resistivity values obtained in the models (Table 4). It is possible to define a range between 5 years and 20 years which matches with the age of the municipal landfill, since it was completely closed at least 5 years before this study was done.

The profiles were located close to the phreatimeters. Table 5 shows the comparison between resistivity measured in the phreatimeters and resistivity determined by the geophysical models at the same point and depth.

The expressions of Meju (2000) were also applied to estimate the electrical conductivity and resistivity of the fluid. The estimated resistivity is significantly lower than the experimental resistivity. This discrepancy can be explained by the presence of several levels of clay, which Meju's equations do not take into account (Table 5).

Additionally, groundwater electrical conductivity measured in the phreatimeters was compared to phreatic aquifer electrical conductivity obtained from the 2D model at the same point and depth. A good lineal correlation was observed between both conductivities. These indicate that the formation factor is almost homogeneous in the aquifer.

Profiles	σb (mS/m) ρb (ohm m)	TDS Predicted (mg/L)	σw Predicted (mS/m)	Cl- Predicted (mg/L)	W Estimate (Vol %)	Age (Year)	Profiles	σb (mS/m) ρb (ohm m)	TDS Predicted (mg/L)	σw Predicted (mS/m)	Cl- Predicted (mg/L)	W Estimate (Vol %)	Age (Year)
Lan01 (a) x = 50M z = 4,5M	169,49 (5,9)	3944,58	568,43	1121,02	52,89	10-20	Lan 01 (b) x = 50M z = 4,5M	169,49 (5,9)	9842,64	1329,28	3106,98	33,82	5-10
Lan 02 (a) x = 50M z = 6M	109,29 (9,15)	2124,89	309,02	539,49	57,86	10-20	Lan 02 (b) x = 50M z = 6M	109,29 (9,15)	4733,25	680,25	1390,60	38,19	10-20
Lan 04 (a) x = 50M z = 5M	135,50 (7,38)	2877,00	416,53	771,92	55,37	10-20	Lan 04 (b) x = 50M z = 5M	185,50 (7,38)	6604,41	944,51	2061,80	35,98	5-10
Lan 14 (a) x = 74,5M z = 4,7M	197,90 (5,05)	4907,87	704,97	1451,46	51,25	10-20	Lan 14 (b) x = 74,5M z = 4,7M	197,90 (5,05)	11878,80	1684,13	4127,17	32,40	0-5
Lan 15 (a) x = 17,4M z = 6,7M	163,99 (6,10)	3765,27	542,97	1061,04	53,25	10-20	Lan 15 (b) x = 17,4M z = 6,7M	163,99 (6,10)	8876,89	1263,96	2924,70	34,13	5-10

Table 4. Hydrochemical parameters calculated for the landfill. The values of minimum electrical resistivity obtained ρ_b were used to predict TDS (a) with equation (1) and (b) with equation (2); the electrical conductivity of fluid is predicted using equation (3) and the chloride content with equation (4); The water content W is estimated applying equation (5) and the years are inferred using the content of TDS and Cl- (Meju, 2000).

Phreatimeter	Profile	Depth (m)	σwm (date) (mS/m), (Month/Year)	ρwm (ohm m)	ρb (ohm m)	ρw Predicted (ohm m) (a) (b)
P1	Lan07	2,15	204,0 (4/05)	4,90	5,75	0,72 - 3,22
P1	Lan12	2,15	136 (12/06)	7,35	9,12	1,46 - 3,22
P2	Lan06	2,10	174,3 (4/05)	5,73	6,90	0,96 – 2,19
P4	Lan09	1,76	267,0 (12/06)	3,74	5,43	0,66 – 1,57
P5	Lan10	1,45	490,0 (12/06)	2,04	3,14	0,29 – 0,73
P6	Lan11	2,00	75,2 (12/06)	13,29	11,63	2,12 – 4,52
P7	Lan11	2,05	123,6 (12/06)	8,09	8,27	1,26 – 2,81

Table 5. Comparison between resistivity measured in phreatimetres (ρ_{wm}) and resistivity determined in geophysical models (ρ_b) at the same point and depth. The last column shows water resistivity applying (a) equation 1 and (b) equation 2

2.3.5 Gualeguaychú landfill conclusions

The 2D models obtained within the landfill show a first layer with high resistivity (100 to 1000 ohm-m) and a thickness of less than 4 meters. This layer hosts the domestic and industrial wastes.

The low resistivity values observed below the wastes which could reach up to 10 m of depth are possibly due to leachate retained in the sediments of the Punta Gorda Group.

The neighbouring areas also have very conductive shallow zones which may be due to the migration of the leachate through groundwater flow or to the lithology of the deposits. At the northern boundary of the landfill a conductivity surface was detected and relatively high values of conductivity were measured in the wells. Some resistive bodies (~100 ohm-m) were found enclosed in a layer with a resistivity in the order of ~15 ohm-m. These anomalies are explained as lithological variations of the Punta Gorda Group.

The eastern boundary of the landfill has a conductive layer located at the same level as the layer inside. This could be due to the contamination at the border of the waste deposit and also by the presence of clays.

The results of GPR profiles showed strong reflectors, where the wastes are deposited and the upper limit of the contaminant plume was identified along the profile by the absence of reflectors or the existence of very weak signals. In this zone, the 2D resistivity model shows the presence of high electrical conductivity materials, which do not allow radar waves to reach greater depths.

The dipole-dipole and GPR results show good agreement and the integrated interpretation, is supported by local geology.

In the most conductive zones below the landfill some hydrochemical parameters of the leachate were predicted applying the empirical relationships defined by Farquhar (1989) and Meju (2000). The fluid conductivity values are in general comparable with the electrical conductivity measured in water surface samples and less than in the water samples from phreatimeters.

2.4 Bariloche Landfill

2.4.1 Background

The landfill of the city of San Carlos de Bariloche is located on National Route 258 (RN 258) approximately 8 km SW. The site was initially used as a place of extraction of materials for the construction of the road (Figure 17). The generated depression was used for disposal of wastes. It is an open dump around 10 hectares area and 8 m to 10 m deep, which began operations in the early 80 s.
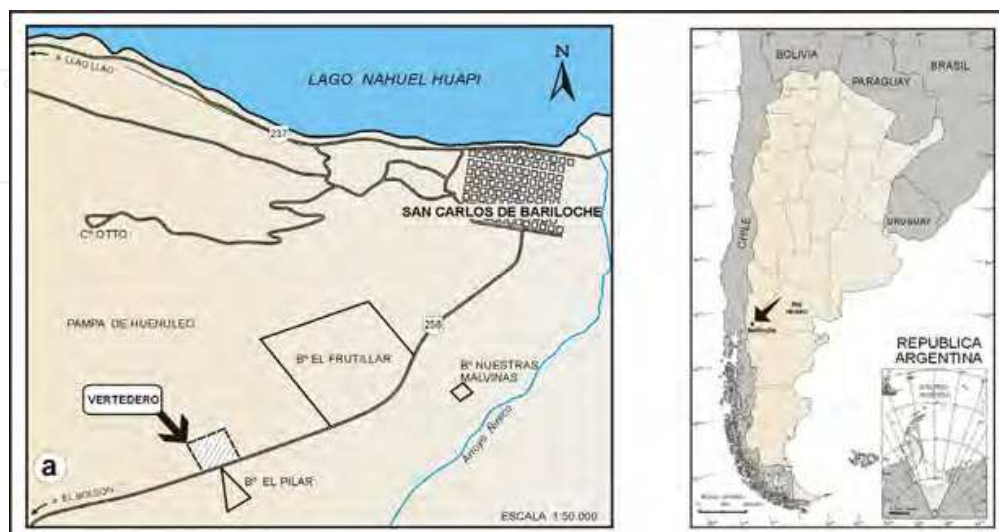

Fig. 17. Location of the Bariloche landfill relevant to the Rio Negro province, Argentina.

The deposition substrate is formed by glacial deposits, highly permeable and with low sorting. It is mainly composed of blocks, gravel and sand. Due to these textural characteristics, leachate has high potential to reach and contaminate the aquifers. Groundwater is the source of drinking water for urban areas adjacent to the repository.

2.4.2 Gelogical and hydrogeological setting

Outcrops present in the area correspond to geological units that comprise the Nahuel Huapi Group of Lower Tertiary age and the sedimentary Complex post-Pliocene-Quaternary which were descript by González Bonorino (1973) and González Bonorino & González Bonorino (1978) and are presented in Table 6.

AGE	UNIT		LITOLOGHY	HYDROGEOLOGIC BEHAVIOUR
LowerTertiary - Quaternary	Sedimentary Complex		Glacial and glacifluvial sediments	Aquifer, high to moderate permeability
Upper Tertiary	Nahuel Huapi Group	Ñirihuau Formation	Feldspar Wackes tuff, etc.	Some aquifer sections located in rocks with fissure porosity Very low permeability
		Ventana Formation	Lavas, brecchias, tobas, etc.	
Premesozoic	Cristalline Basament		Igneous and metamorphic rocks	Aquiclude

Table 6. Stratigraphic column

The landfill is located on sediments of the Sedimentary Complex post-Pliocene Quaternary, which also form a watershed and are part of the recharge zone of at least three major aquifer systems. These aquifer systems and related channels provide drinking water to urban areas nearby. Figure 18 shows a picture of the area.

Fig. 18. A photo of the landfill landscape

2.4.3 Field work

In the study area more than 30 GPR profiles were performed (Figure 19) reaching depths between 10 m and 40 m and 4 electrical tomographies using the DD configuration. DD1 and DD2 profiles were located within the landfill and DD3 and DD4 outside of it. Profiles DD1, DD2 and DD4 were oriented in the same direction (NW-SE), while the DD3 is almost perpendicular to them (see location in Figure 19).
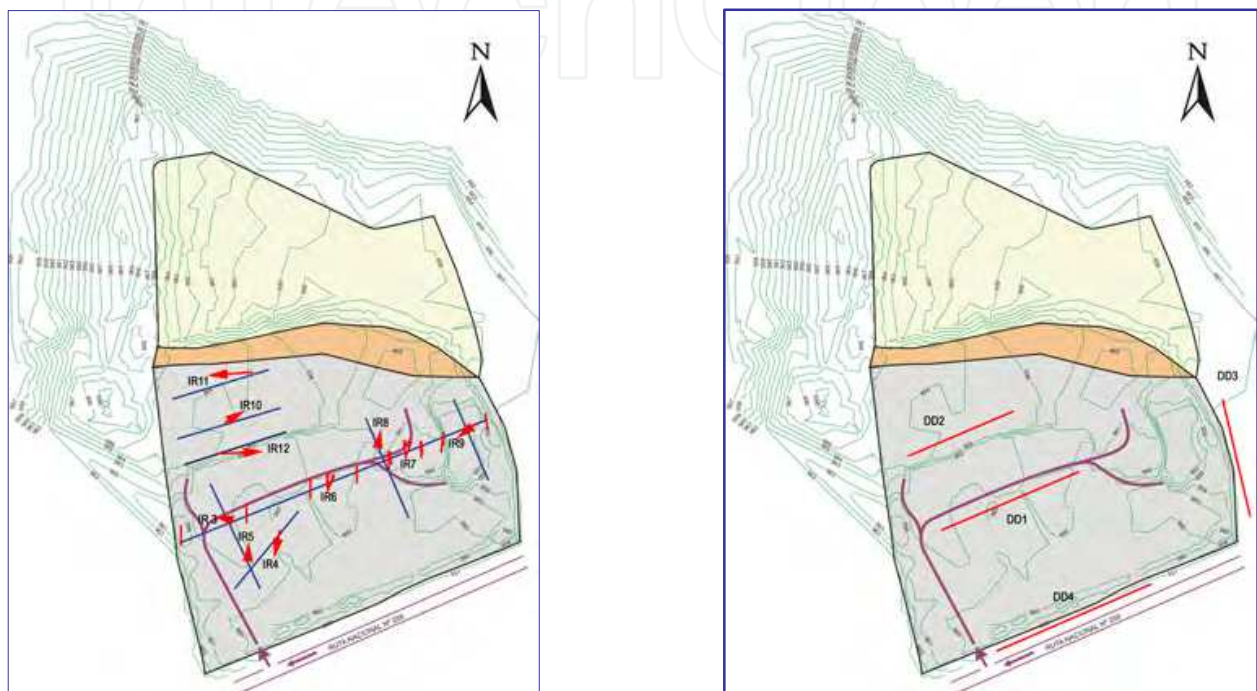

Fig. 19. A schematic map showing location of: a) GPR profiles; b) Geoelectrical profiles: DD1, DD2, DD3 y DD4.

2.4.4 Results and discussion

The lowest electrical resistivity obtained in the different models is about 1 ohm-m, while the highest is near the 10000 ohm-meters. These four orders of magnitude difference allowed the detection in the landfill areas of conductive anomalies which can be interpreted as groundwater contamination by leachate and the average resistivity of the ground outside of the landfill indicates the direction of flow of leachate.

Models of DD1 and DD2 profiles show variations in the electrical resistivity from 1 ohm-m to 1000 ohm-m (Figure 20 and 21). In both cases, the first 3 m - 4 m are very resistive. This layer represents the waste deposit and shows heterogeneity typical of areas with higher air content. These resistivity anomalies could be indicating the maximum depth of the deposit. Below the waste the resistivity values range from 20 ohm-m to 60 ohm-m reaching depths around 7 m to 12 m and the more conductive zones observed up to 20 m deep especially at the ends of the two profiles could be due to the presence of leachates. In the case of DD2 profile, where the anomaly is more extended, this could be explained by the uncontrolled discharging of waste fluids.
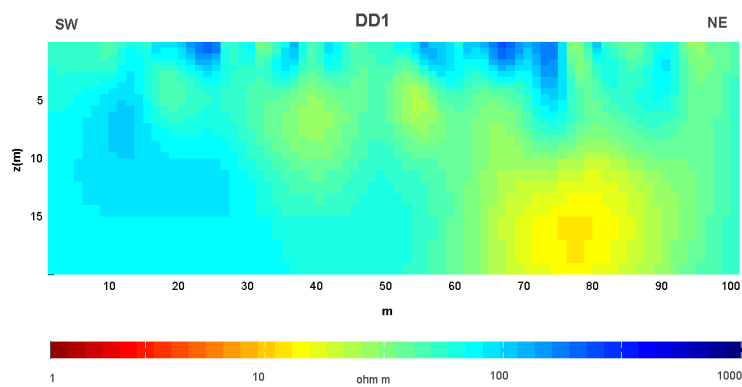
Fig. 20. 2D resistivity model up to 20 m deep obtained within the landfill (DD1).
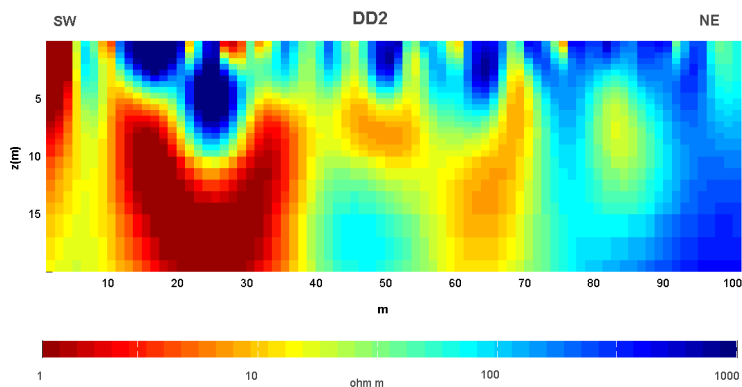

Fig. 21. 2D resistivity model up to 20 m deep obtained within the landfill (DD2).

Models of the DD3 and DD4 profiles show that the resistivity of the shallow layer for both cases is about 5000 ohm-m - 2000 ohm-m, but below 10 m deep the minimum resistivity is around 200 ohm-m for DD3 while in DD4 the resistivity anomaly is below 20 ohm-meters (see Figures 22 and 23).
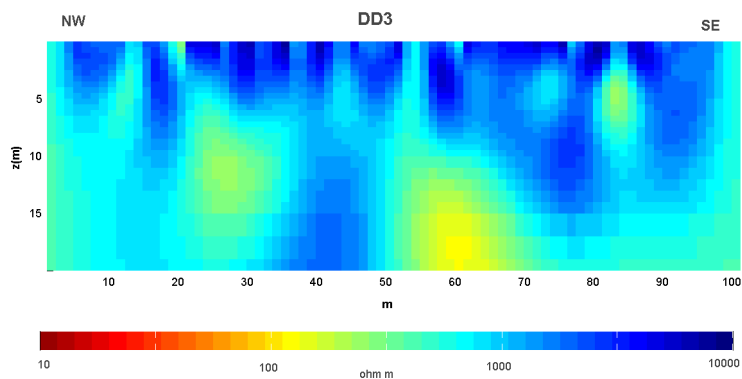

Fig. 22. 2D resistivity model up to 20 m deep obtained outside the landfill (DD3).
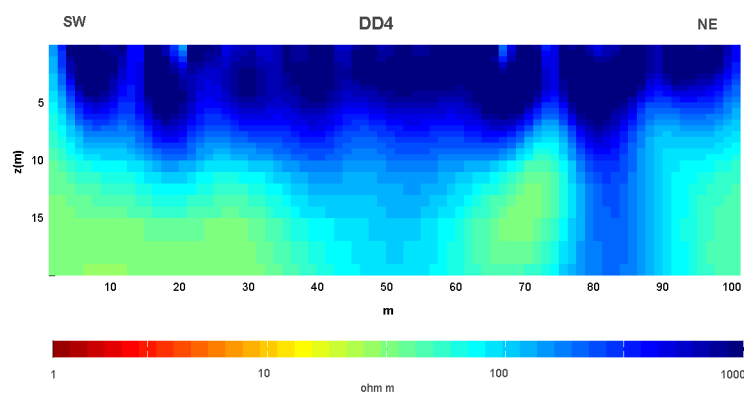
Fig. 23. 2D resistivity model up to 20 m deep obtained outside the landfill (DD4).

This behaviour suggests that the leachate could be migrating to this area (RN 258) and contaminating it corresponding to the DD4 profile. The zone corresponding to DD3 profile is uncontaminated. This is an important conclusion, because it coincides with the general idea of the flow direction provided by previous investigations.

Analysis of the GPR profiles has shown the characteristics of the fill, which is irregular in thickness, layout and compaction. Figure 24 presents the radar image of IR4 with 150 Mhz antenna showing the structure of the filling to a depth of 3 m and distinguishes the presence of an object buried at shallow depths.
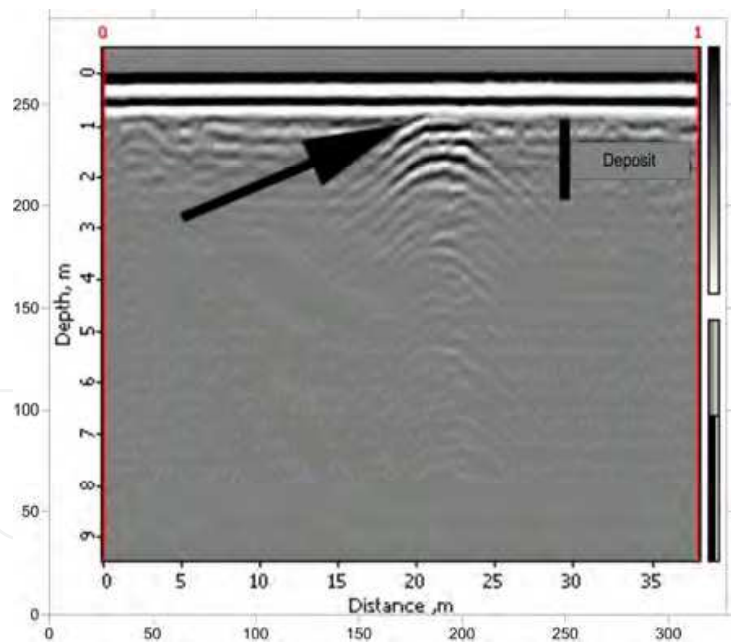
Fig. 24. Radar image for the landfill up to 9 m of depth.

2.4.5 Bariloche Landfill conclusions

In summary, this study reflects the existence of an irregular filling with variable depths between 5 m and 7 m, with a maximum depth estimated of 12 meters. The presence of leachate, recognizable to a depth of around 20 m - 25 m, suggests that levels are not impermeable so as to prevent the migration of leachate into the subsoil. The contamination

plume moves towards to the RN 258, there is no recorded evidence of its displacement in NE direction.

Electrical resistivity models obtained are characteristic of landfills with large resistivity contrasts due to the presence of highly conductive fluids and waste which are usually resistive. These results have been correlated with images obtained with GPR. Also, the presence of buried objects of considerable size, associated with piece of metal, oil drums, amongst other things, has been detected.

3. Conclusion

In both cases studied, geoelectrical methods and ground penetrating radar have shown that they are efficient techniques for identifying contamination plumes produced by waste disposal sites due to their high salinity.

These non-invasive geophysical methods proved to be useful in terms of detecting and mapping physical-chemical changes associated with the presence of wastes. These methods do not require drilling and so avoid the risk of further contamination of the surface and groundwater.

Geological, hydrogeological and hydrochemical data are required to complement the geophysical results providing a more complete interpretation.

The application of this methodology is promising for use in environmental impact assessments of sanitary landfills which are the most common way to eliminate solid urban wastes.

4. Acknowledgements

5. References

Bell, F. G. & Jermy, C. A. (1995). A seepage problem associated with an old landfill in the greater Durban area. In: Sarsby, R.W. (Ed.). *Waste Disposal by Landfill GREEN'93*: 607–614. A.A. Balkema, Rotterdam.

Birks, J. & Eyles, C. A. (1997). Leachate from landfills along the Niagara Escarpment. En: Eyles, N. (Ed.). *Environmental Geology of Urban Areas. Geological. Associaiton of Canada*, Chap. 24: 347–363. Canada.

Buselli, G., Barber, C., Davis, G. B. & Salama, R. B. (1990). Detection of groundwater contamination near waste disposal sites with transient electromagnetic and electrical methods. En: Ward, S.H. (Ed.). *Geotechnical Environmental Geophysics*. Vol. 2: 27-39. SEG Publ, Tulsa, OK.

Bobachev, A., Modin, I. N. & Shevnin V. (1990-2000). Software. Department of Geophysics. Geological Faculty. Moscow State University y Geoscan-M. Ltd.

Daniels, D. (2004). Ground Penetrating Radar. 2nd Edition. *IEE Radar, Sonar and Navigation Series*, 15, 726 pp.

Farquhar, G. J. (1989). Leachate: production and characterisation. *Canadian Journal of Civil Engineering* 16: 317–325.

Fili, M. (2001). Síntesis geológica e hidrogeológica del noroeste de la provincia de Entre Ríos – República Argentina. *Boletín Geológico y Minero,* Vol 112, Número especial: 25-36. ISSN 0366-0176. Madrid.

Iriondo, M. M. (1980). El Cuaternario de Entre Ríos. *Ciencias Naturales del Litoral, Revista* N° 11: 125-141, Santa Fé. Argentina.

González Bonorino, F. (1973). Geología del área entre San Carlos de Bariloche y Llao Llao, provincia de Río Negro. Departamento Recursos Naturales y Energía, *Fundación Bariloche*, Publicación 16: 53p.

González Bonorino, F. & González Bonorino, G. (1978). Geología de la región de San Carlos de Bariloche: Un estudio de las Formaciones Terciarias del Grupo Nahuel Huapi. *Asociación Geológica Argentina, Revista* XXXIII (3): 175-210.

Loke, M.H. (1999). Time-lapse resistivity imaging inversion. *Proceedings of the 5th Meeting of the Environmental and Engineering Geophysical Society European Section, Em1.*

Meju, M. (2000). Geoelectrical investigation of old abandoned, covered landfill sites in urban areas: model development with a genetic diagnosis approach. *Journal of Applied Geophysics* 44: 115–150.

Oldenburg, D. W., McGillivary, P. R. & Ellis, R. G. (1993). Generalized subspace method for large scale inverse problems. *Geophysics* V.114, p.12-20. 1993.

Oldenburg, D. W. &Li, Y. (1994). Inversion of induced polarization data. *Geophysics* V59: 1327-1341.

Radar System, Inc. Software Prism. (2004). http://www.radsys.lv.

Pomposiello, C., Favetto, A., Boujon, P., Dapeña, C. & Ostera, A. (2008). Evaluación del estado actual de sitios de disposición final de residuos sólidos urbanos aplicando técnicas geofí-sicas. *Revista de Geología Aplicada a la Ingeniería y al Ambiente*. Vol 22 123-133. ISSN 1851-7838.

Pomposiello, C., Dapeña, C., Boujon, P. & Favetto, A. (2009). Tomografías eléctricas en el basurero municipal ciudad de Gualeguaychú, provincia de Entre Ríos, Argentina. Evidencias de contaminación. *Asociación Geológica Argentina, Revista* 64 (4) 603-614.

Prezzi, C. Orgeira, M. J., Vásquez, C. J. A & Ostera, H. (2005). Groung Magnetic of a municipal solid waste landfill: pilot study in Argentina. *Environ. Geol.* 47: 889-897.

Radar System, Inc., 2004. Software Prism. http://www.radsys.lv.

Russo, A., Ferello, R. E. & Chebli, G. (1979). Cuenca Chaco Pampeana. En: Geología Regional Argentina, II Simposio de Geología Regional Argentina. *Academia Nacional de Ciencias de Córdoba,* Vol. I (4): 139-183. Córdoba.

Yaramanci, U. (1994). Relation of in situ resistivity to water content in rock salts. *Geophysical Prospecting* V. 41, p. 229–239.
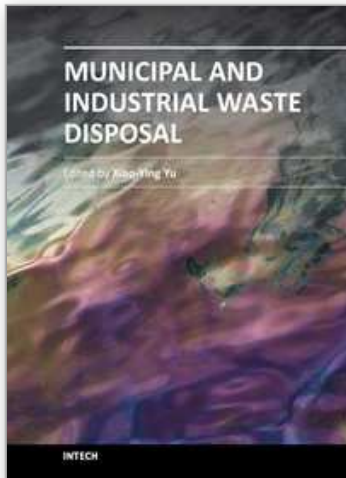
Municipal and Industrial Waste Disposal

Edited by Dr. Xiao-Ying Yu

This book reports research findings on several interesting topics in waste disposal including geophysical methods in site studies, municipal solid waste disposal site investigation, integrated study of contamination flow path at a waste disposal site, nuclear waste disposal, case studies of disposal of municipal wastes in different environments and locations, and emissions related to waste disposal.

How to reference

In order to correctly reference this scholarly work, feel free to copy and paste the following:

Cristina Pomposiello, Cristina Dapeña, Alicia Favetto and Pamela Boujon (2012). Application of Geophysical Methods to Waste Disposal Studies, Municipal and Industrial Waste Disposal, Dr. Xiao-Ying Yu (Ed.), ISBN: 978-953-51-0501-5, InTech, Available from: http://www.intechopen.com/books/municipal-and-industrial-waste-disposal/application-of-geophysical-methods-to-waste-disposal-studies-

INTECH
open science | open minds